

# Permittivity of Sub-Soil Materials Retrieved through Transmission Line Model and GPR Data

Claudia Guattari\*, Davide Ramaccia, Filiberto Bilotti, and Alessandro Toscano

**Abstract**—In this paper, we propose a new retrieval technique to estimate the dielectric permittivity of the sub-soil materials of a stratified structure. The core of the retrieval procedure is a proper electromagnetic circuit model representing the realistic stratified media as a cascade of transmission line segments. Exploiting the analogies between the electrical parameters of the transmission line segments and the constitutive parameters of the materials of the multilayer structure, the propagation of the Ground Penetrating Radar (GPR) signal is equivalently represented as a pair of voltage and current waves propagating in the transmission line network. The effectiveness of the proposed retrieval technique is confirmed by proper experimental results. In particular, the retrieved electromagnetic parameters of the sub-soil materials are found to be consistent with the ones obtained by a direct characterization of the same materials. These results suggest that the proposed method can be successfully applied to the material characterization able to monitor several macroscopic properties of sub-soil materials.

## 1. INTRODUCTION

In the last decades, the Ground Penetrating Radar (GPR) has been established as one of the most important tools in a great variety of scientific, research and technical areas for the study of underground water detection, geotechnical and civil engineering, glaciology, and archeology [1,2]. Several papers related to GPR theory, technology, and applications are focused on the ability of the GPR to give a representation of the underground, exploiting the propagation and the reflection of electromagnetic waves. However, this operation provides an erroneous time-to-depth conversion because the propagation velocity of the electromagnetic signal in the underground is generally assumed to be constant, as if the underground is composed just by one uniform semi-infinite medium, leading to a unrealistic representation of the underground stratigraphy.

This limitation has not been ignored by the scientific community that in the last years had intensely worked on this topic. In fact, the electromagnetic echo recorded by GPR is due to the different electromagnetic parameters (i.e., effective relative permittivity, permeability and conductivity) of the materials along the stratification [3], whose knowledge leads to a correct time-to-depth conversion and a correct estimation of the depth of a buried target [2]. Moreover, the knowledge of the dielectric permittivity of soil allows to infer the chemical, physical and mineralogical properties of the mixture composing the soil, being a macroscopic parameter related to the soil moisture content [4–6], to the mixture density of asphalt [7], and to the air voids per unit of volume [8].

In this framework, it is possible to find many different techniques for estimating the dielectric permittivity of the soil by using the raw time-domain GPR data. As an example, some of these techniques are based on the use of a reference buried target placed at a known depth [9], on proper comparisons of the amplitudes of the received signal peaks [10, 11], or more complex and time-consuming methods, such as the one based on the Green's function [12].

---

*Received 20 February 2015, Accepted 3 April 2015, Scheduled 16 April 2015*

\* Corresponding author: Claudia Guattari (claudia.guattari@uniroma3.it).

The authors are with Department of Engineering, "Roma Tre" University, Via Vito Volterra 62, Rome 00146, Italy.

In this paper, we present a simple and effective retrieval procedure based on an analytical model of the stratified soil that can be used in conjunction with any commercial GPR system. A stratified soil, such as an highway road pavement, an archeological area, a geological stack of sedimentary rocks, are constituted by a layered deposition of different materials and, thus, can be studied as a microwave circuit consisting of a cascade of different transmission line segments [13–20]. The analogies between the realistic scenario of a stratified medium and the microwave circuit open the doors to an innovative way to analyze the GPR signal, returning a complete description of the propagation effect of the GPR electromagnetic pulse in presence of a generic scenario.

Here we analytically derive the reflection coefficient of the entire stratified structure, which takes into account the contribution of each layer to the propagation of the GPR signal (assumed to be described by their effective relative permittivity and thickness). The analytical received signal and the GPR one are, thus, compared for estimating the electrical parameters of the layers constituting the stratified soil. The effectiveness of the proposed model is tested through proper numerical simulations [21] and direct characterization of the involved materials in the waveguide measurement setup.

## 2. ANALYTICAL TRANSMISSION LINE MODEL

### 2.1. Equivalent Circuit Model of a Stratified Soil

Let us consider a stratified structure consisting of  $N$  layers of different materials placed between two semi-infinite media, A and B, as shown in Figure 1(a). Each layer is infinitely extended in  $x$ - and  $y$ -directions, whereas in  $z$ -direction the thickness of  $i$ -th layer is indicated with  $d_i$ . Assuming non-magnetic and lossless materials, the electromagnetic behavior of each layer is described only by its relative permittivity  $\varepsilon_r$ . In this case, we will consider that the electromagnetic source is a uniform monochromatic plane-wave normally impinging on the material interfaces from medium A (see Figure 1(a)). The electric and magnetic field vectors, orthogonal to the propagation direction  $z$ , are parallel to the interfaces of the stratified medium, and the impinging plane wave is, thus, a TEM one. The incident wave propagates with different phase velocities inside the layers of the stratified medium

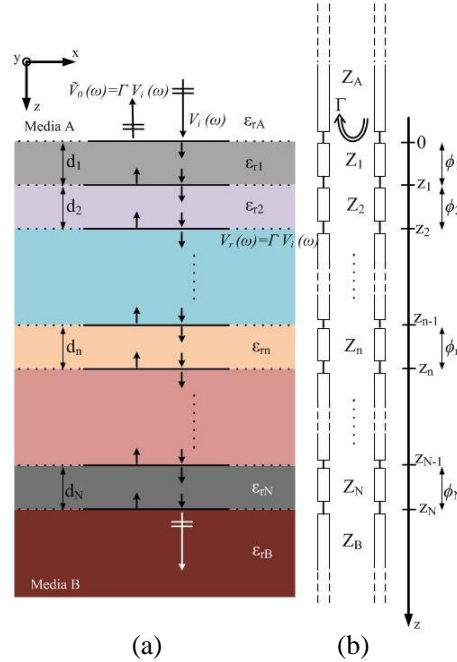


**Figure 1.** (a) Section view of a generic stratified media consisting of  $N$  layers between two semi-infinite media. (b) Its equivalent transmission line model. An uniform TEM plane-wave is impinging the structure from media A.

and at each interface, in order to satisfy the boundary conditions, part of the energy is reflected back, propagating along the negative  $z$ -direction.

As well-known from electromagnetic field theory, the propagation along such a medium can be described in circuital terms as the propagation of a TEM wave along a cascade of transmission line segments (see Figure 1(b)), whose key parameters are the characteristic impedances  $Z$  and the propagation constants  $\beta$  [13]. Of course, such parameters change when the permittivity of the layers changes.

Exploiting the analogy reported in Figure 1, the frequency response of the stratified medium can be easily evaluated by solving the corresponding circuit equations. The characteristic impedance and the electrical length of the  $i$ -th transmission line segment in Figure 1(b) can be expressed as:

$$\begin{aligned} Z_i &= Z_0 / \sqrt{\varepsilon_{r,i}} \\ \phi_i &= \beta_i d_i \end{aligned} \quad (1)$$

where  $Z_0$  is the characteristic impedance of vacuum, i.e., 377 Ohm,  $\varepsilon_r$  the relative electric permittivity of the layer, and  $\beta$  the propagation constant of the electromagnetic field in the layer. The propagation constant is related to the angular frequency  $\omega$  of the monochromatic incident field according the relationship:

$$\beta_i = \frac{\omega}{c} \sqrt{\varepsilon_{r,i}} \quad (2)$$

where  $c$  is the speed of light in vacuum. Following the microwave circuit theory, the reflected and transmitted signals by the  $N$  transmission line segments can be related to the incident one by using the reflection and transmission coefficients, respectively. In order to relate the reflected and transmitted signals to the incident one, the  $2 \times 2$  matching matrix  $[MM]$  and propagation matrix  $[PM]$  of any layer have to be evaluated as follows:

$$[PM]_i = \begin{bmatrix} e^{-j\phi_i} & 0 \\ 0 & e^{-j\phi_i} \end{bmatrix}; \quad [MM]_{i,i+1} = \frac{1}{\tau_{i,i+1}} \begin{bmatrix} 1 & \rho_{i,i+1} \\ \rho_{i,i+1} & 1 \end{bmatrix} \quad (3)$$

where  $\tau_{i,i+1}$  and  $\rho_{i,i+1}$  are the Fresnel coefficient between the  $i$ -th layer and the next one:

$$\begin{aligned} \tau_{i,i+1} &= \frac{2Z_{i+1}}{Z_{i+1} + Z_i} \\ \rho_{i,i+1} &= \frac{Z_{i+1} - Z_i}{Z_{i+1} + Z_i} \end{aligned} \quad (4)$$

The relationship between the complex magnitude of a monochromatic field at the input port, i.e., the incident and the reflected ones, and the one at the output port, i.e., the transmitted field, can be written as:

$$\begin{bmatrix} E_i \\ E_r \end{bmatrix} = \left( [MM]_{A,1} \cdot \sum_{i=1}^N [PM]_i [MM]_{i,i+1} \right) \begin{bmatrix} E_t \\ 0 \end{bmatrix} \quad (5)$$

where the term  $[MM]_{N,N+1} = [MM]_{N,B}$ .

The backward propagating signal in medium B vanishes due to its infinite extension. Solving Eq. (5) for the unknowns  $E_r$  and  $E_t$ , the reflection and transmission coefficients of the entire stratified structure are:

$$\Gamma = \frac{E_r}{E_i}; \quad T = \frac{E_t}{E_i}; \quad (6)$$

It is worth noticing that both coefficients depend only on the geometrical thickness  $d$ , the electric permittivity  $\varepsilon_r a$  of the layers and on the angular frequency of the electromagnetic excitation. If we consider a given stratified structure, the reflection and transmission coefficients in magnitude and phase can be evaluated over a certain frequency range, varying the frequency value in the Expression (6), leading to the complex spectrum of the reflected and transmitted signals, which, thus, can be written as:

$$\begin{aligned} \tilde{E}_r(\omega) &= \Gamma(\omega) \tilde{E}_i(\omega) \\ \tilde{E}_t(\omega) &= T(\omega) \tilde{E}_i(\omega) \end{aligned} \quad (7)$$

The time-domain reflected and transmitted signals,  $E_r(t)$  and  $E_t(t)$ , can be easily evaluated applying the inverse Fourier transform to the corresponding complex spectra  $\tilde{E}_r(\omega)$  and  $\tilde{E}_t(\omega)$ . In particular, we are interested to  $E_r(t)$ , which the signal measured by the GPR.

## 2.2. Numerical Validation

In order to validate the analytical transmission line model, we make a comparison between the analytical results and the numerical ones obtained by a proper set of full-wave simulations performed with CST Microwave Studio [21]. Without loss of generality, we report here the comparison of the complex reflection coefficient over a normalized broad frequency range for a stratified structure consisting of a stack of only three layers of materials placed between two semi-infinite media. Referring to Figure 1, the semi-infinite medium A is just air ( $\varepsilon_{rA} = 1$ ), whereas the relative permittivities of the other materials are:  $\varepsilon_{r1} = 7.5$ ,  $\varepsilon_{r2} = 10$ ,  $\varepsilon_{r3} = 18$ ,  $\varepsilon_{rB} = 6.5$ . The thicknesses of the three layers are:  $d_1 = 0.2\lambda_0$ ,  $d_2 = 0.5\lambda_0$ , and  $d_3 = 0.8\lambda_0$ .

In Figure 2, we report amplitude and phase of the reflection coefficient evaluated at the air-ground interface. The analytical and numerical results agree quite well over a 100% fractional bandwidth, which is the typical bandwidth of a GPR system [2]. This comparison confirms that the proposed analytical model can be successfully employed for the retrieval of the effective permittivity of the sub-soil materials, by a making a comparison between the real GPR data and the analytical ones (i.e., the synthetic GPR data) obtained through (7).

In the following Section, we present a retrieval algorithm based on this analytical method and capable to determine the effective permittivity of the sub-soil materials.

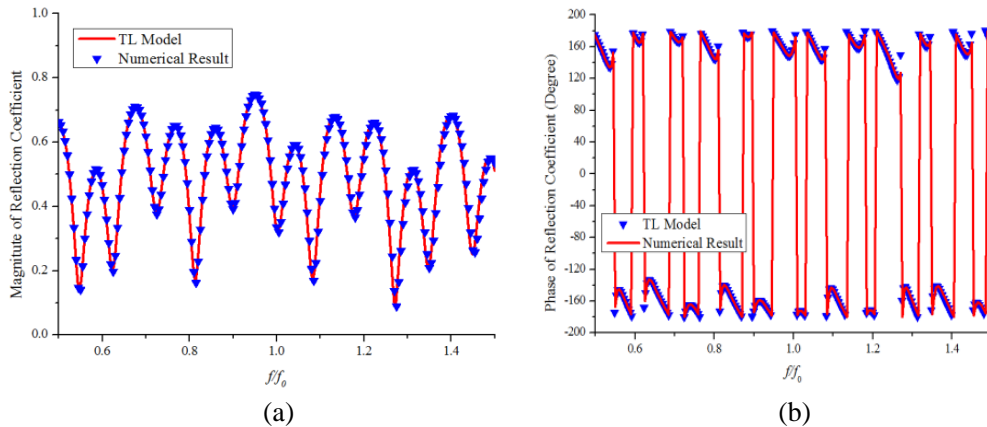


**Figure 2.** Comparison of the reflection coefficient at  $z = 0$  obtained by using the TL model and the full-wave simulator: (a) magnitude and (b) phase.

## 3. RETRIEVAL PROCEDURE AND EXPERIMENTAL VERIFICATION

The proposed retrieval technique starts with the acquisition of two signals from the GPR: the first one is obtained in a regular operating condition by placing the GPR on the stratified medium while the second one is obtained when the GPR is flipped towards the free-space, as reported in [22, 23]. During the acquisitions, no obstacles should be present over and/or in proximity of the GPR antennas. In this way, we get a scaled copy of the signal launched by the GPR generator towards the ground, whatever the GPR system is. In the following, we refer to these two time-domain signals as the reference signal  $v_0(t)$  (over the stratified medium) and the input signal  $v_i(t)$  (in free-space), respectively.

The second stage consists of the synthesis of an artificial GPR signal, denoted as  $\tilde{v}_0(t)$ , by using the circuit model proposed in this work and described in the following subsection. Such synthetic signal is a function of the electric permittivity of each layer. Therefore, in order to find the optimum set of estimated values of the relative permittivity, the synthetic signal can be compared to the reference

signal  $v_0(t)$  obtained from the direct GPR survey. The retrieval procedure is formulated in terms of a classical least square problem: the quantity  $\bar{D}_2$  is the mean quadratic deviation between the real and the synthetic GPR time-domain signal

$$\bar{D}_2 = \frac{1}{T} \int_0^T [v_0(t) - \tilde{v}_0(t)]^2 dt \tag{8}$$

which has to be minimized by finding the proper set of the electromagnetic parameters  $\{\epsilon_{r1}, \epsilon_{r2}, \dots, \epsilon_{rn}, \dots, \epsilon_{rN}\}$  which describe the electromagnetic properties of the common road, an airport pavement, an archeological area or a geological stack of sedimentary rocks under investigation.

Here we analyze the pavement of a real airport taxiway in Italy. The picture of an extracted core of the taxiway reported in Figure 3 clearly reveals the stratified nature of the pavement under investigation. It consists of three different materials: hot-mix asphalt (HMA, top layer), concrete (middle layer) and soil (bottom layer semi-infinite space). The electromagnetic behavior of each layer is described only through the relative permittivity of the materials, whereas the thicknesses of the two finite layers are  $d_1 = 120$  mm and  $d_2 = 270$  mm, respectively. As already discussed in the first part of the Section, since the taxiway is characterized by a multilayered structure, it can be easily modeled through using a proper equivalent transmission-line circuit representation, as shown in Figures 4(a)–(b).

In this study, we used a commercial Ground Penetrating Radar, manufactured by IDS S.p.A. Italy, equipped with Hi-Mod ground-coupled radar antennas (RIS/MF system) (Figure 4(c)). In according to the aforementioned procedure, we have performed two measurements: one in free-space and one on the road pavement. Then, in order to estimate the three relative permittivity values of the materials under investigation, we evaluated the goal function  $\bar{D}_2$  in three different steps. In the first one, only the interface air-HMA is considered, i.e., two infinitely extended media with permittivity  $\epsilon_{r.air} = 1$  and  $\epsilon_{r.HMA}$ , respectively. Changing the value of  $\epsilon_{r.HMA}$  we minimized the error function  $\bar{D}_2$  at  $\epsilon_{r.HMA} = 8$  (dark-gray line in Figure 5(a)). Then, we considered the presence of the second material, and we evaluated again the error function  $\bar{D}_2$  varying the permittivity of the second layer, i.e.,  $\epsilon_{r.conc}$ , when  $\epsilon_{r.HMA} = 8$ . The new minimum of  $\bar{D}_2$  was reached for  $\epsilon_{r.conc} = 15.0$  (light-gray line in Figure 5(a)). Finally, we considered the third material with the other two permittivity already set and we minimized the error function  $\bar{D}_2$  at  $\epsilon_{r.soil} = 15.2$  (orange line in Figure 5(a)). By using the retrieved values, we compare the synthesized GPR signal obtained by the transmission line model presented in Section 2.1 and the one obtained by the GPR experimental survey. It is possible to note from Figure 5(b) that the agreement between the two time-domain signal is very good.

In order to further demonstrate the reliability of the proposed technique, we compare these effective permittivity values with the ones obtained by direct measurements of the materials in an electromagnetic waveguide [24]. The waveguide measurement setup consists of two segments of regular electromagnetic waveguides connected to a sample holder filled with a material sample, as shown in Figure 6. Port 1 and

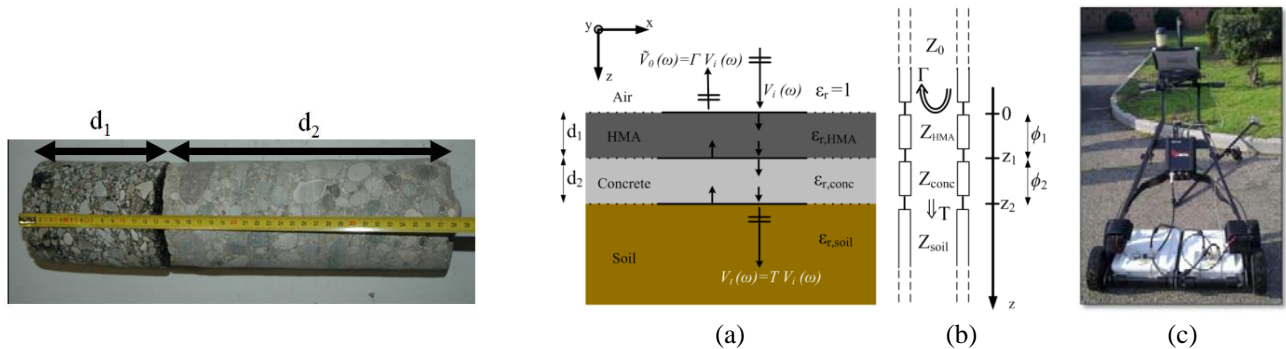


**Figure 3.** Extracted core from the airport taxiway pavement: the first layer is hot-mix asphalt and the second one is concrete.

**Figure 4.** (a) Section view of airport taxiway consisting of two layers between air and soil; (b) equivalent transmission-line circuit model; (c) picture of used Ground Penetrating Radar.

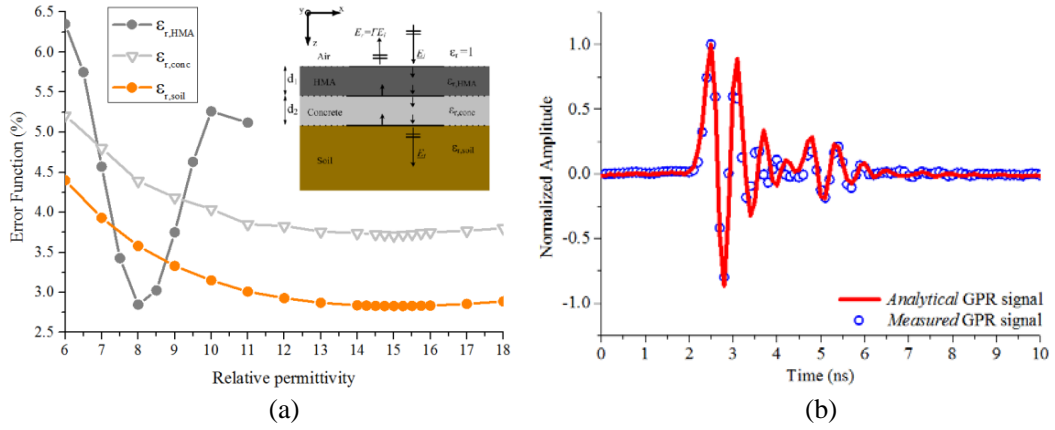


**Figure 5.** (a) Percentile mean-squared error  $E$  for each layer. (b) Comparison between analytical and measured GPR signal in time domain. The analytical signal is evaluated using the retrieved electromagnetic parameters.

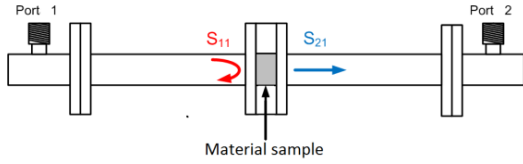


**Figure 6.** Waveguide measurement setup. Port 1 and Port 2 are connected to a VNA and the material sample is extracted from the core shown in Figure 3.

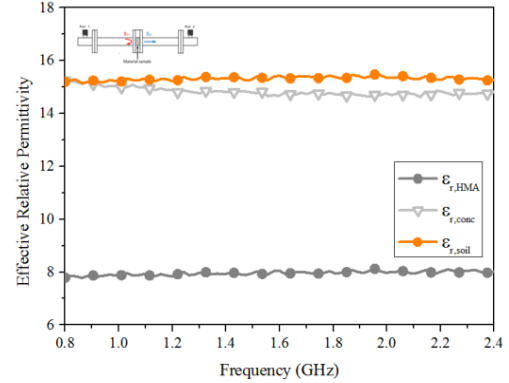


**Figure 7.** Values of the effective relative permittivity of HMA, concrete and soil within the GPR frequency band.

Port 2 are connected to the Vector Network Analyzer Rohde & Schwarz ZVB-14 [25] that, after a proper calibration process, is able to measure the complex reflection and transmission coefficients of the material sample, i.e., the scattering parameter  $S_{11}$  and  $S_{21}$ , respectively, over the same frequency band of the used GPR (800–2400 MHz). From these data it is possible to extract the effective electrical permittivity of the individual materials [24] reported in Figure 7. As evident, such values are in a good agreement with the ones predicted by employing the proposed analytical equivalent circuit model, demonstrating, thus, that the proposed approach represents a step towards non-destructive electromagnetic characterization of the sub-soil materials.

#### 4. CONCLUSION

In this paper, we present a novel procedure to retrieve the constitutive parameters of a stratified soil, based on an equivalent transmission-line circuit model of a stratified medium. The proposed retrieval procedure is applied with success to infer the electromagnetic parameters of the stratified pavement of a real airport taxiway. The method is able to find the optimal electromagnetic values that are in good agreement with the expected results for the three different analyzed materials: HMA, concrete and soil. Moreover, the analytical circuit model is able to generate a realistic synthetic GPR signal

due to the ability of the transmission-line mode to take into account any transmission and reflection effects during the propagation of the electromagnetic wave in a stratified medium. It is shown that the analytical and real GPR signals are very similar when the proper values of relative permittivity and thickness of each layer are implemented. Moreover, these results are compared to the ones obtained by direct measurements in a regular waveguide. The good agreement between these two sets of data demonstrates the reliability of the method that can be considered a step forward towards a noninvasive dielectric characterization of stratified materials.

## REFERENCES

1. Jol, H. M., Ed., *Ground Penetrating Radar: Theory and Applications*, 1st Edition, Elsevier Science, Amsterdam, 2009.
2. Daniels, D. J., *Ground Penetrating Radar*, 2nd Edition, IEEE Press, 2004.
3. Orfanidis, S. J., *Electromagnetic Waves and Antennas*, 2008, Online Book Available at: <http://www.ece.rutgers.edu/~orfanidi/ewa>.
4. Topp, C. G., J. L. Davis, and A. P. Annan, "Electromagnetic determination of soil water content: measurements in coaxial transmission lines," *Water Resources Research*, Vol. 16, No. 3, 574–582, 1980.
5. Lunt, I. A., S. S. Hubbard, and Y. Rubin, "Soil moisture content estimation using ground penetrating radar reflection data," *Journal of Hydrology*, Vol. 307, 254–269, 2005.
6. Lambot, S., E. Slob, D. Chavarro, M. Lubczynski, and H. Vereecken, "Measuring soil surface water content in irrigated areas of southern Tunisia using full-waveform inversion of proximal GPR data," *Near Surface Geophysics*, 403–410, 2003.
7. Leng, Z., I. L. Al-Qadi, and P. Shangguan, "Field application of ground penetrating radar for asphalt mixture density measurement: A case study of Illinois Route 72 overlay," *Transportation Research Board 91st Annual Meeting*, 133–141, Washington, DC, Jan. 22–26, 2012.
8. Al-Qadi, I. L., Z. Leng, S. Lahouar, and J. Baek, "In-place hot-mix Asphalt density estimation using ground penetrating radar," *Transportation Research Board 89th Annual Meeting*, 19–27, Washington, DC, Jan. 10–14, 2010.
9. Walker, P. D. and M. R. Bell, "Subsurface permittivity estimation from ground-penetrating radar measurements," *2000 Radar Conference*, 341–346, Alexandria, VA, May 7–12, 2000.
10. Giannopoulos, A. and N. Diamanti, "A numerical investigation into the accuracy of determining dielectric properties and thickness of pavement layers using reflection amplitude GPR data," *Int. Conf. on Ground Penetrating Radar*, 655–658, Delft, The Netherlands, Jun. 21–24, 2004.
11. Liu, H. and M. Sato, "Robust estimation of dielectric constant by GPR using an antenna array," *2011 IEEE International Geoscience and Remote Sensing Symposium*, 178–181, Vancouver, BC, Jul. 24–29, 2011.
12. Minet, J., S. Lambot, E. Slob, and M. Vanclooster, "Soil surface water content estimation by full-waveform GPR signal inversion in the presence of thin layers," *IEEE Trans. Geoscience Remote Sensing*, Vol. 48, No. 3, 1138–1150, Mar. 2010.
13. Pozar, D. M., *Microwave Engineering*, 4th Edition, John Wiley & Sons, New York, 2011.
14. Ramaccia, D., F. Scattone, F. Bilotti, and A. Toscano, "Broadband compact horn antennas by using EPS-ENZ metamaterial lens," *IEEE Trans. Ant. Propag.*, Vol. 61, No. 6, 2929–2937, Jun. 2013.
15. Bilotti, F., L. Di Palma, D. Ramaccia, and A. Toscano, "Self-filtering low-noise horn antenna for satellite applications," *IEEE Ant. Wireless Propag. Lett.*, Vol. 11, 354–357, 2012.
16. Ramaccia, D., L. Di Palma, G. Guarnieri, S. Scafè, A. Toscano, and F. Bilotti, "Balanced and unbalanced waveguide power splitters based on connected bi-omega particles," *Electronics Lett.*, Vol. 49, No. 24, 1504–1506, Nov. 2013.
17. Ramaccia, D., L. Di Palma, D. Ates, E. Ozbay, A. Toscano, and F. Bilotti, "Analytical model of connected bi-omega: Robust particle for the selective power transmission through sub-wavelength apertures," *IEEE Trans. Ant. Propag.*, Vol. 62, No. 4, 2093–2101, Apr. 2014.

18. Ramaccia, D., F. Bilotti, and A. Toscano, "Analytical model of a metasurface consisting of a regular array of sub-wavelength circular holes in a metal sheet," *Progress In Electromagnetics Research M*, Vol. 18, 209–219, 2011.
19. Ramaccia, D., A. Toscano, and F. Bilotti, "A new accurate model of high-impedance surfaces consisting of circular patches," *Progress In Electromagnetics Research M*, Vol. 21, 1–17, 2011.
20. Ramaccia, D., C. Guattari, F. Bilotti, and A. Toscano, "Metamaterial split-ring resonators for retrieval of soil electromagnetic properties," *Proc. of Metamaterials' 2013*, 1–3, Bordeaux, France, Sep. 16–21, 2013.
21. CST Studio Suite, 2015, [www.cst.com](http://www.cst.com).
22. Nishimoto, M., K. Tomura, and K. Ogata, "Waveform calibration of ground penetrating radars for identification of buried objects," *IEICE Trans. Electron.*, Vol. 95-C, No. 1, 105–109, Jan. 2012.
23. Nishimoto, M., D. Yoshida, K. Ogata, and M. Tanabe, "Extraction of a target response from GPR data for identification of buried objects," *IEICE Trans. Electron.*, Vol. 96-C, No. 1, 64–67, Jan. 2013.
24. Bogle, A., M. Havrilla, D. Nyquis, L. Kempel, and E. Rothwell, "Electromagnetic material characterization using a partially-filled rectangular waveguide," *Journal of Electromagnetic Waves and Applications*, Vol. 19, No. 10, 1291–1306, 2012.
25. Rohde & Schwarz, VNA ZVB-14, URL: <http://www.rohde-schwarz.it/product/ZVB.html>.